General Disclaimer

One or more of the Following Statements may affect this Document

- This document has been reproduced from the best copy furnished by the organizational source. It is being released in the interest of making available as much information as possible.

- This document may contain data, which exceeds the sheet parameters. It was furnished in this condition by the organizational source and is the best copy available.

- This document may contain tone-on-tone or color graphs, charts and/or pictures, which have been reproduced in black and white.

- This document is paginated as submitted by the original source.

- Portions of this document are not fully legible due to the historical nature of some of the material. However, it is the best reproduction available from the original submission.

UCSD-SP-79-04

Infrared Continuum Observations of the Solar Atmosphere

FINAL REPORT

NSG-7100

by

H. Hudson, P. LeVan, C. Lindsey

March 1979

ABSTRACT

The far-infrared wavelengths (10 μm - 1 mm) have been used to study the spatial and temporal structure of the solar atmosphere. Observational results were obtained on flares, faculae, sunspots, and on the center-to-limb intensity distribution, as well as on time variability within these regions. A program of precise monitoring of slow variations in the integrated solar luminosity was shown to be feasible, and initial steps to implement observations were completed.

PAPERS PUBLISHED WITH SUPPORT FROM NSG-7100

1. "Direct Observation of Temperature Amplitude of Solar 300-sec Oscillation", by H.S. Hudson and C.A. Lindsey, Ap.J. (Lett.), 187, L35,(1974).
2. "Submillimeter Observations of Planets", by H.S. Hudson, C.A. Lindsey, and B.T. Soifer, Icarus, 23, 374 (1974).
3. "The Solar-Flare Infrared Continuum", by K-I. Ohki and H.S. Hudson, Solar Phys., 43, 405 (1975).
4. "The Solar-Flare Infrared Continuum: Observational Techniques and Upper Limits", by H.S. Hudson, Solar Phys., 45, 69 (1975).
5. "An Infrared Continuum Study of the Solar Atmosphere", by C.A. Lindsey, Ph.D. Dissertation, UCSD (1975).
6. "Solar Limb Brightening in Submillimeter Wavelengths", by C.A. Lindsey and B.T. Soifer, Icarus, 23, 374 (1974).
7. "Infrared Continuum Observations of Solar Atmospheric Structure", by C.A. Lindsey, Solar Phys., 52, 263 (1977).

FINAL REPORT, NSG-7100

Infrared Continuum Observations of the Solar Atmosphere

H. Hudson, P. LeVan, C. Lindsey

I. INTRODUCTION

The sun is the brightest object in the sky at all wavelengths between ~ 10 cm and $\sim 10^{-8}$ cm, and we have accumulated considerable knowledge (summarized by White, 1977) in all spectral ranges. Nevertheless, striking gaps in observational knowledge occur frequently, and these necessarily correspond to ignorance of the physical conditions best described by the missing data. The infrared wavelengths (defined as 1 μ - 1 mm for the purposes of this report) are the most prominent example. Very little observational work has taken place, especially on the various forms of solar activity.

The infrared continuum forms in the upper photosphere under normal conditions, with wavelength increasing with height up to "submillimeter" wavelength, $300\ \mu < \lambda < 1$ mm, in the vicinity of the temperature minimum. The minimum opacity of the solar atmosphere, just longward of the H^- recombination continuum, also occurs in the infrared band at $\sim 1.6\ \mu$. The infrared wavelengths cover the entire lower solar atmosphere in one continuous variation of a single source of opacity, namely H^- free-free absorption.

The observational program in the solar infrared at UCSD has two main phases: the exploration of the fine structure of the solar atmosphere, and the measurement of the infrared variability of the sun viewed as a star. We describe results from the high-resolution program in Section II; these

include information on many types of atmospheric structures. Section III then reviews solar variability, Section IV describes the infrared observational approach, and Section V observational results. The measurement of infrared variability, especially at long periods, is a continuing program at UCSD.

II. SOLAR INFRARED WORK AT UCSD - HIGH RESOLUTION

A. Temperature Structure of Photosphere

The high-resolution infrared work done at UCSD has exploited both the near infrared atmosphereic transmission windows and those at submillimeter wavelengths. Although the transmission at submillimeter wavelengths is more highly affected by the water vapor content of the atmosphere (even at dry, high sites such as Mount Lemmon Observatory, Arizona), these far-infrared wavelengths nevertheless probe a different layer of the solar atmosphere, and are thus indispensible in providing clues as to the response of the different layers, particularly when simultaneous measurements at two distinct wavelengths are made and compared.

(1) Nature of the transmission windows selected.

The 10, 18, and 26 micron passbands used in UCSD solar infrared work are determined primarily by the helium-temperature filters. In addition, the earth's atmosphere also provides a filtering effect on the solar radiation from O_3 and especially H_2O absorption bands. As indicated in Table 1, passbands are $\sim$ 10%. For the 10, 18, and 26 μ passbands the effective wavelength does not depend strongly upon atmospheric conditions.

On the contrary, transmission at submillimeter wavelengths is strongly affected by atmospheric water content. The few discrete windows between 350 μ and 1 mm have transmissions that depend strongly on the H_2O vapor content. The longer wavelength bands are those most strongly degraded by high water vapor content. For this reason, when a long-pass filter is used which admits all bands beyond 350 microns, the effective center wavelength of the resulting transmission is shifted to shorter wavelengths with higher atmospheric water vapor content. For details see Hudson et al., 1974.

(2) Height of formation

As mentioned in the introduction, the different wavelengths used in UCSD solar work were chosen to study different layers of the sun's atmosphere. The exact height above the visible photosphere at which the different wavelengths originate is called the height of formation. In reality, the region of formation is roughly confined to a layer approximately one scale height in thickness and with a sharp low-altitude cutoff (Figure 1). The formation heights for the wavelengths of 10 microns - 1 millimeter extend from about 200 to 1000 kilometers above the photosphere. These values were calculated (Lindsey, 1976) from the solar atmospheric parameters of the Harvard-Smithsonian Reference Atmosphere (Gingerich et al., 1972). Thus, by using the filtering schemes described previously, one should in theory be able to study the solar atmosphere at the different altitudes corresponding to the maxima of these contribution functions. The presence of inhomogeneities in the solar atmosphere rules out a simple model for height of formation, however, because of the finite angular beamwidth of

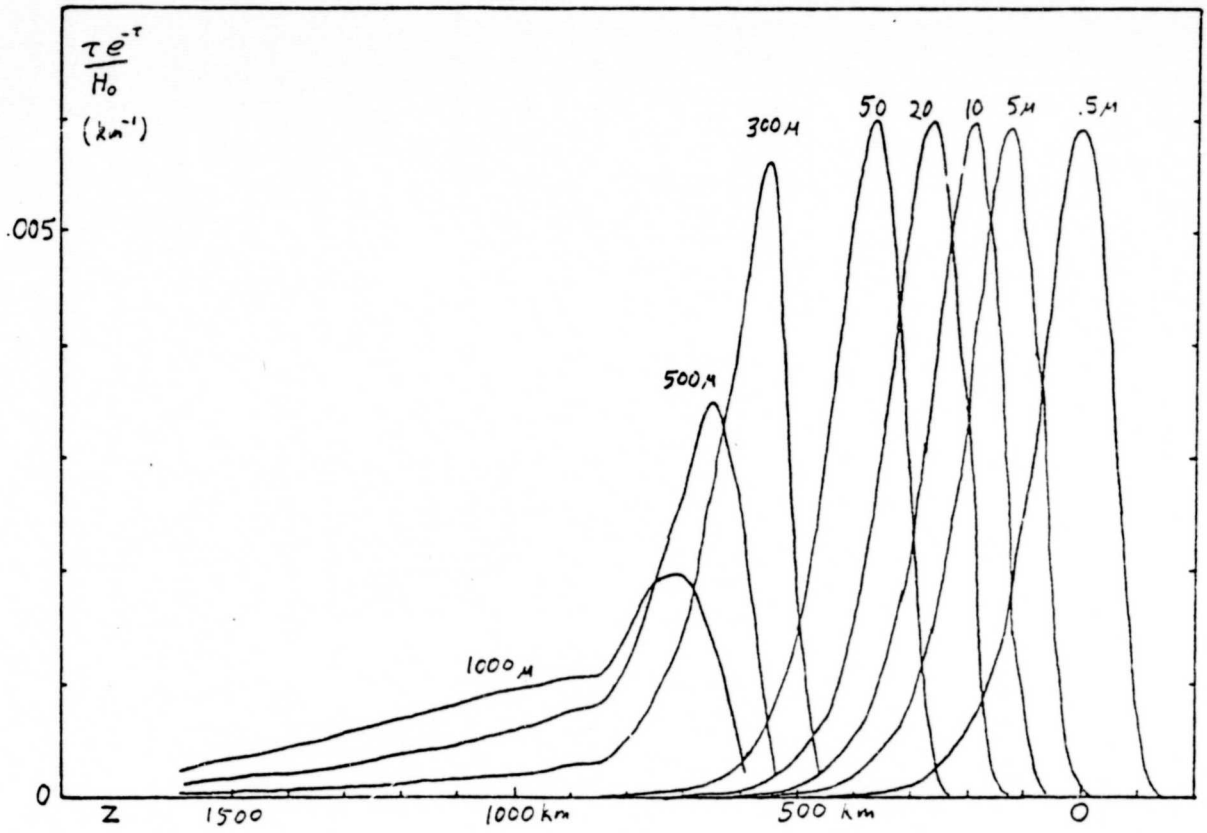

Figure 1. Contribution functions estimated for infrared radiation between 5 μ and 1 mm wavelengths. C is defined by

$$C \equiv - T(z) \frac{d\tau}{dz} e^{-\tau} \quad .$$

Since τ varies about exponentially with height

$$\frac{d\tau}{dz} \simeq - \frac{1}{H_o} \tau \quad ,$$

where H_o is the e-folding height for τ. Thus

$$C \simeq \frac{T(z)}{H_o} \tau e^{-\tau} \quad ,$$

and since $T(z)$ varies slowly compared to τ, we have plotted simply

$$\hat{C} = \frac{\tau e^{-\tau}}{H_o} \quad .$$

the photometric measurements (Table 1). This is especially the case for the upper photosphere where submillimeter wavelengths are used.

(3) Selected wavelengths and resolution.

The Mount Lemmon telescope has a 1.52 meter primary reflecting surface, and a corresponding diffraction-limited resolution of about one arc minute at 350 microns. Such an angular scale corresponds to approximately 45,000 kilometers on the solar surface. In comparison the characteristic sizes of granulation, supergranulation, faculae, sunspots, flares, filaments, surges, etc. are all considerably smaller. For this reason, detailed studies of structures are confined to the lower photosphere and made with near infrared wavelengths. The resulting beam width can be decreased to 10 arc sec without restriction by diffraction. By chopping two 10 arc sec beams separated by several arc min, one may effectively subtract any fluctuations in atmospheric transmission which may otherwise adversely affect the radiative photometry. The effectiveness of this technique is due to the small spatial separation between the two beams in the earth's atmosphere; at 5 arc min angular separation the corresponding linear separation at a distance of 1.6 kilometers is 2 meters, a distance comparable to the telescope diameter. The two beams thus largely overlap and sample approximately identical atmospheric paths.

(4) Mapping.

A high signal-to-noise ratio is easily attained with standard astronomical infrared detectors (Low-type bolometers) and the use of two-

TABLE 1

Spectral Response for Solar Infrared Photometry

λ microns	$\Delta\lambda$ microns	h_{HSRA} km	FWHM arc sec
10.1	1.3	130	10
17.9	1.4	210	10
26	2	290	10
510*	220*	900*	82*

*Values calculated for line-of-sight water vapor content of 1 mm (Hudson et al., 1974).

beam photometry as discussed above. Abundant spatial variability appears at all wavelengths, as indicated by the data shown in Fig. 2. Such structure is obviously related to sunspots and faculae, within active regions, and in quiet sun areas the spatial variations have an oscillatory time structure. A modest limb darkening appears (Johnson, 1971; Lindsey, 1976), as can be seen in the full-disk 22 μ scan in Fig. 3; the large deflections in the scan occur when one of the beams begins to detect sky signal. The slope is essentially the gradient of the solar signal at regions within the field of view of the beams as one progresses across the solar diameter.

In addition to the quiet sun structure described above, the 5 arc min beam separation permits the monitoring of regions with steep intensity gradients against the constant background of one beam in a relatively quiet zone. Scans made through sunspot regions (Fig. 2) record brightness temperature deficits according to the size of the sunspot group.

(5) Solar flares.

The original purpose of the solar infrared photometry was to search for solar flares. The infrared continuum should be enhanced during flares from a variety of mechanisms (Ohki and Hudson, 1975). No flares were positively detected during extensive observations correlated with the Skylab mission; we report upper limits in Table 2 (Hudson, 1975). The basic single reason for the lack of flare detections is the solar-minimum level of activity during the observations. We strongly recommend that observations be resumed during more active conditions.

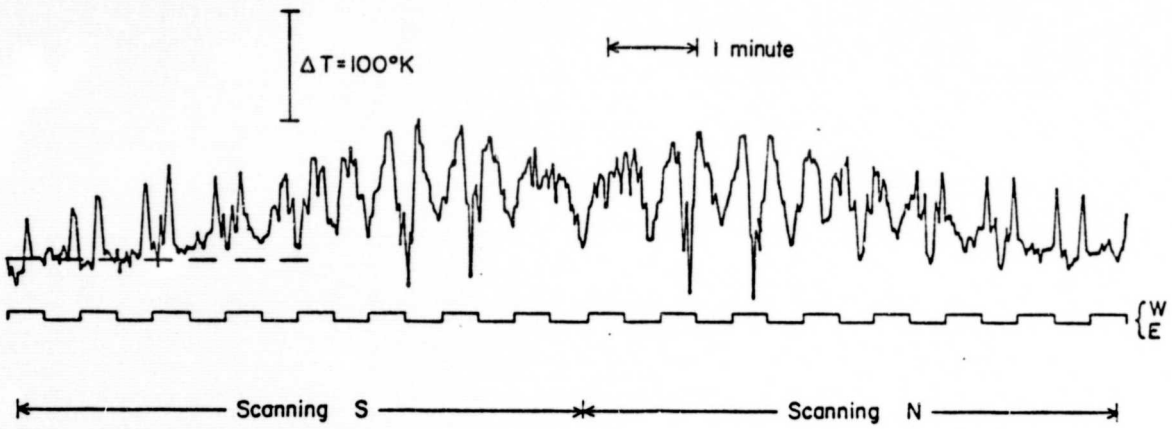

Figure 2. Example of raster scanning with an 11" beam at 20 μ: McMath region 10300, December 19, 1973. The square wave shows the pattern of EW scans comprising the raster, which covers an area ∿ 3 × 3' in ∿ 8 min. The dashed line indicates a quiet-Sun level, with upward deflections corresponding to positive excesses in the signal beam. Sunspots caused the negative signals, but were unresolved under the conditions of this raster scan. The large extent of the active-region excess-flux is interesting, as is the degree of reproducibility in consecutive (adjacent) scans.

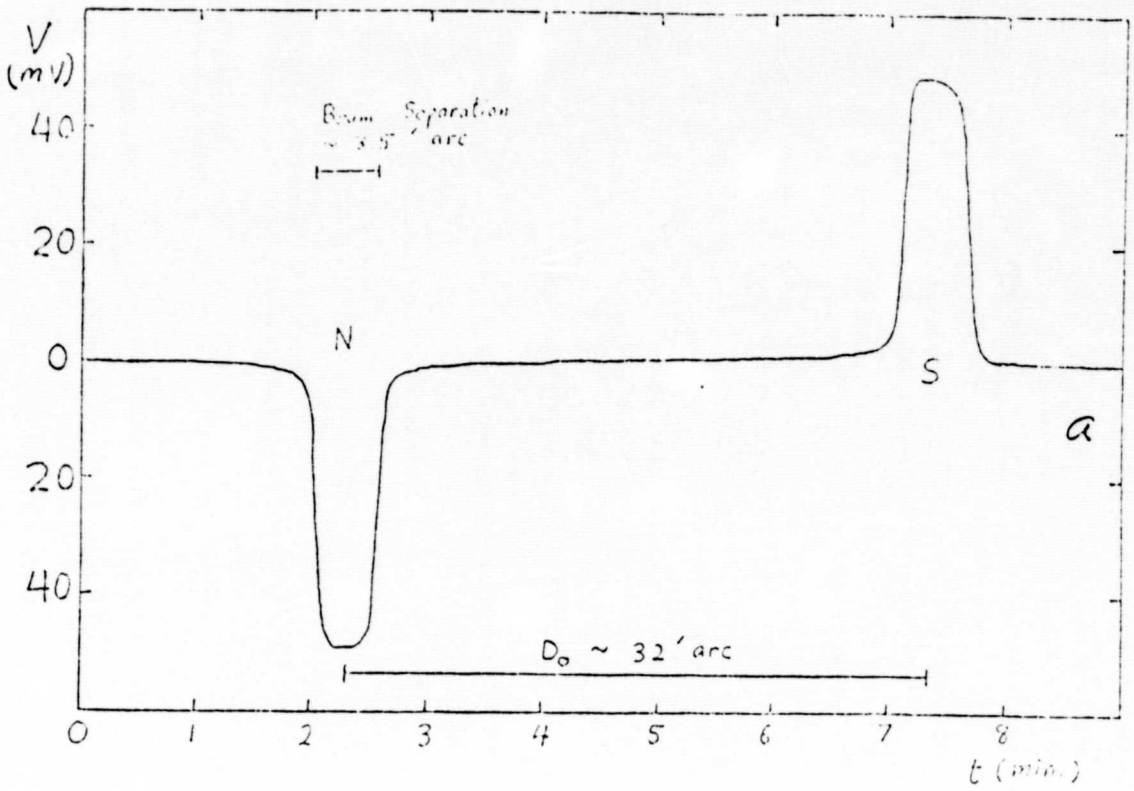

Figure 3. (a) Two-beam scan of the sun at 22 μ. The beam separation was 3.5 arc min, and the scan rate was about 6.5 arc min/minute. The angular resolution, defined by a 1 mm aperture, was about 10 arc sec. The vertical axis shows the difference in signal between the two beams in millivolts as determined by the lock-in amplifier from the output of a detector preamplifier.

The negative excursion at $\sim$ 2.2 minutes from the start of the scan (t = 0) and the positive excursion at $\sim$ 7.3 minutes are the sections during which respectively, the south beam only, and the north beam only, were on the sun, the other looking at the sky. The region between is the well-cancelled section in which both beams were on the sun and their respective signals subtracted. A slightly positive gradient throughout this mid-section reveals a small radial darkening over the entire disk.

(b) Sketch of the reconstructed intensity profile.

TABLE 2

Threshold of Sensitivity of Infrared Observations

Window	Mode	Burst Duration	Minimum Detectable Burst	
			ΔT °K	Flux Density [W $(m^2$ Hz$)^{-1}$]
350 μ	Monitor	Impulsive	30	3×10^{-22}
350 μ	Monitor	Gradual	100	10^{-21}
18 μ	Monitor	Impulsive	5	6×10^{-20}
18 μ	Monitor	Gradual	15	2×10^{-19}
18 μ	Scan	Gradual	5	6×10^{-21}

(6) Supergranulation-related effects in the upper photosphere.

A study was undertaken to look for structure in the photosphere whose size and brightness fluctuations would resemble those of the supergranulation known to exist in the convective region. Sample scans of one arc min length were made at 26 micron wavelength over a period of about 30 seconds, for a total of 4 minutes observing time. Averaging techniques employed yielded a mean value for the size scale of the observed variations, which corresponds reasonably well with the 30,000 kilometer scale of a typical supergranule. Direct analysis of the long-period variable of the signal (which would correspond to supergranulation) was made difficult by the presence of a more rapidly varying component with spatial extent of about 10,000 kilometers. The determined rms spatial amplitude of the longer-period variable was found to be well below estimates derived from observations at optical wavelengths of the corresponding phenomena (Lindsey, 1976).

(7) Nature of the observed short-period components.

The occurrence of short-period variability in the infrared continuum was first recognized during this program (Hudson and Lindsey, 1974). The nature of the variation has been investigated in the wavelength region described earlier and conclusions regarding their spatial extent, period, and amplitude have been drawn. The work of different wavelengths has given information about the height dependence of the oscillating structures.

In order to determine the extent of the correlation of the variability in different layers of the solar atmosphere, simultaneous observations at different wavelengths were undertaken. The combinations of wavelengths were 10 and 26 microns, 10 and 22 microns, 10 and 18 microns, and 10 and 13 microns. The correlation in the last combination was found to be very high; we attribute this to the overlap of the contribution functions at 10 and 13 microns, as expected. Particularly interesting features resulted from the 10 and 26 micron comparison; these wavelengths do not have this overlap of contribution functions. The power spectrum of the 22 micron sample showed a 2.5 °K rms excess in the 2.9 to 4.8 MHz frequency band, but this "5-minute oscillation" feature is smaller at 10 microns. The similarity in appearance of the 10 micron power spectrum to that of the visible continuum as measured by Edmonds et al. (1965) along with the near equality of the magnitude of the rms brightness temperature variations in the two spectral regions when corrected for differences in beam diameter, indicate that the atmospheric layer responsible for the 10 micron radiation follows closely the temperature variations of the white-light photosphere.

On the other hand, the radiative relaxation times for the layers where the 10 and 26 micron radiation originate are about 30 and 100 seconds, respectively (data taken from Gibson, 1973). Compressional waves of the frequencies noted above elicit different responses from the two layers, due to the differing characteristic radiation times. The growth of temperature amplitude with height is only crudely known from these data, but Noyes and Hall (1972) inferred an amplitude ~ 250 K near the temperature minimum.

III. VARIABILITY OF THE SUN, VIEWED AS A STAR

A. Five Minute Velocity Oscillations

The detection of solar velocity field oscillations of an approximate five minute periodicity was accomplished by Leighton (1962) and other groups through Doppler shift analysis of solar spectral lines. Certain characteristics of the oscillations are well determined while others are under recent investigation due to prior observational discrepancies.

(1) Observed Characteristics

The period originally determined by Leighton, using a photographic subtraction technique in which solar atmospheric velocities appear as brightness differences in the light originating from opposite sides of a spectral line, was 296.1 ± 1.3 seconds. This value made using the low-lying Ca λ6103 line, is more precise than those values obtained from lines whose formation heights are higher in the solar atmosphere, where the resonant peak of the oscillation is considerably broadened. The suggestion that two or more discrete periods may be present was made by Frazier

(1966, 1968), who suggested that the shorter component may become more important with height in order to account for the broadening of period with altitude.

The lifetimes of individual bursts have been determined to be of about twenty-minute duration, through analysis of the bandwidths of the resonant peaks in the power spectra. The lifetimes are height-dependent -- chromospheric and photospheric lifetimes were determined to be fourteen and thirty-one minutes, respectively (Bhattacharyya, 1972).

The horizontal scale of the oscillations is the most underdetermined of all the measured parameters. Leighton's original determination of 1700 and 3500 kilometers for lower and higher altitude size scales respectively is smaller than later measurements which range from 3000 to 7000 kilometers (Evans and Michard, 1962; Frazier, 1968b; Howard, 1967). Suggestions were made that incomplete removal of solar granular velocities, which are important in the lower regions of the photosphere where Leighton's velocity measurements were made, led to the reduced horizontal scale.

(2) Velocity amplitudes

One finds an increase in the velocity amplitude with height in the solar atmosphere, as would be expected by energy conservation (constancy of $\frac{1}{2}\rho v^2$ and decreasing mass density with altitude). The amplitude of the velocity is principally radial as evidenced by the decreased Doppler shift (line-of-sight velocity) toward the solar limbs (Evans and Michard, 1962; Howard, 1967).

(3) Propagation of oscillations

The use of solar spectrograms, which allow simultaneous comparison of spectral lines at different wavelengths and formation heights, can afford a determination in the delay time of wave propagation between two distinct atmospheric layers. Evanescent wave motion is suggested by the report of thirty seconds delay between layers of 200 kilometer separation (Jensen and Orrall, 1963) which implies a phase velocity less than the sound speed. Observations made deeper in the photosphere of brightened temperature and velocity amplitude phase differences indicate propagating wave character, however.

B. Possible Mechanisms for Generation and Selection of Five-Minute Velocity Oscillations

The solutions to the equations of motion which describe wave propagation in a gravitationally stratified, isothermal atmosphere give vertical wave number values ($k_z = 2\pi/\lambda$, z: vertical direction in stratified atmosphere) in terms of frequency and the horizontal wave number. Alternately, values in w vs. $k_{horizontal}$ space corresponding to constant k_z can be plotted in a diagnostic diagram. The diagram is divided into regions of higher and lower frequency by the non-propagating region in which $k_z^2 < 0$ (pure imaginary) corresponding to acoustic and gravitational wave propagation, respectively. The range of frequency values near the boundaries are in the five minute range, leading to suggestions of possible wave generation and selection of a resonant period.

One possible mechanism for resonant period selection and generation would require the overlapping of a spectrum of generated lower frequency waves with frequencies admitted by a high pass filter acting in upper atmospheric layers. The generation of waves by turbulent motions in the convective region has been considered, but observations of the five-minute velocity resonance deep in the photosphere have discredited this theory.

Because the solar atmosphere is not isothermal as assumed in derivations leading to the diagnostic diagram, certain theories postulate the entrapment of waves of given frequency and wave number within boundaries beyond which increasing temperature at higher altitudes or increasing pressure deeper in the atmosphere would no longer allow propagation. An acoustic wave trapping model proposed by Bahng and Schwarzchild (1963) would require a diminished velocity amplitude in the low photosphere which is observationally not present.

Gravity wave entrapment models (Uchida, 1965, 1967) generalized to non-isothermal atmospheres (Thomas et al., 1971) have yielded resonant periods of 263 and 338 seconds with the shorter period component coming increasingly more into play with altitude, such that the observational decrease in period with altitude is well matched.

Other models of acoustic wave confinement to the convective region of the sun (Leibacher and Stein, 1971) and resulting photospheric motions are supported by the observations of large velocity amplitudes in lower regions of the solar photosphere.

Models in which overstability of waves of certain frequencies and wave numbers result due to the phase lag between the driving and dissipative forces present (Ulrich 1970)generalized to non-radial acoustic modes (Wolff, 1972b, 1973) lead to a discussion of longer period waves whose existence is not confirmed and which are an object of much current research.

C. Longer Period Oscillations

Non-radial oscillatory modes have been studied in conjunction with polytropic stars (Cowling, 1941) and later generalized (Ledoux and Walraven, 1958). Current interest in their application to solar variability is due primarily to the range of periods which they predict (which includes oscillations in the 5 minute range) and to the problems associated with the standard solar model, such as the observed deficiency in the neutrino flux from the solar core. It has been suggested (Dilke and Gough 1972; Christensen-Dalsgaard et al., 1974) that an instability of the core to longer period (~ 1 hour) modes could result in chemical mixing in the inner regions of the sun and lowered neutrino flux. Analysis of the non-radial modes indicates a division similar to that obtained in the radial case in which the lower frequency, longer period waves (> 1 hour) are gravitational in nature, while those of shorter period are due to the compressibility of the solar atmosphere and resemble acoustic waves. Both types of waves are characterized by the number of radial nodes and the order of the associated spherical harmonic surface distortion.

Observations of long-period oscillations have been provided by Sererny, Kotov, and Tsap (1976) over long observing sequences and with care to eliminate any atmospheric source of variation. They report a period of 2 hour and 40 minute duration.

Brookes, Isaak, and van der Raay (1976) have found resonances in their solar power spectra at periods of $2^{hr}\ 40^{min}$, 58^{min}, and 40^{min}, using a resonant scattering device in which scattering atoms subject to a laboratory magnetic field scatter light originating from opposite wings of a solar spectral line. The light from the two wings is polarized differently and Doppler velocity comparisons are made.

Hill et al. (1976), whose technique allows precise determination of solar disk velocities, found numerous peaks in power spectra in the 10 to 50 minute range, but the disk velocity amplitudes associated with these periods are disproportionally larger than those of Brookes et al.

A search for continuum brightness changes with simultaneous monitoring of solar carbon line C I 5380 in the 5 to 60 minute range (Livingston et al., 1977) resulted in no significant variations of brightness temperature at 0.4 °K or greater, indicating perhaps that the continuum responds sluggishly to non-radial oscillation.

In summary the observational results on longer-period oscillation are ambiguous. The refinement and development of new observational approaches continues, however, because the potential rewards of successful detection of oscillation is so great. Dittmer (1977) has provided a comprehensive discussion of the field.

IV. INFRARED MONITORING AND TECHNIQUES

A. Advantages of the 10 Micron Window

We have chosen the ten micron atmospheric window to monitor solar spectral irradiance for a number of reasons. Most important of these is that atmospheric transmission is high (typically 98% and greater at high observation sites). The attenuation of solar flux due to aerosol scattering should be negligible at these longer infrared wavelengths. Variable constituents of the atmosphere (ozone, for example) responsible for absorption can be eliminated in favor of water vapor in suitable wavelength regions. The ability to observe atmospheric water vapor content through use of a spectral hygrometer should then give an indication of the total absorption at any given gime. Sky emissivity at ten microns is high, permitting a quick determination of the atmospheric emission coefficient by scanning over a range of zenith angles. As suggested by F. C. Gillett, emissivity variations in the same spectral band can in principle be used to monitor extinction variations. Finally, the height of formation in the solar atmosphere of the ten micron continuum is very near that at optical wavelengths, and a strong coupling of ten micron flux with total solar luminosity is expected.

B. Dewar Configuration

The heart of the infrared photometer used for solar monitoring consists of a PbSnTe photovoltaic detector cooled to liquid nitrogen temperature and shielded from all but entrance window radiation by

another, independent nitrogen reservoir and flask (Figure 4). The interference filter used has a passband of less than 1 micron and is also kept at liquid nitrogen temperatures, insuring that its thermal radiation will be a negligible part of any measured signal. The current use of a large diameter, short focal length BaF_2 lens permits large, negligible diffraction apertures while limiting the detector field of view to about four times the angle subtended by the solar disk. Thus, solar measurements are made without an excessive amount of sky background.

The electronics configuration consists of a simple DC preamplifier as shown in Figure 5. The inherent stability of operation of the photovoltaic detector is quite good, and gain calibration may be accomplished by the blackbody reference shown in Figure 4.

The operational amplifier used in the circuit was selected for the small temperature drifts of input offset current and voltage (typically 15 pico amps/°C and 0.5 microvolts/°C, respectively). Such small drift coefficients make for drifts in output of less than one millivolt per degree temperature change (see discussion under "Dewar Stability").

C. Dewar Stability

Temperature drifts of isolated components composing the infrared photometer have been checked in the laboratory and subsequently modified when appreciable. The filter was found to be an extremely sensitive component due to the transmission passband dependence on thickness characteristic of interference filters. Small expansions of linear

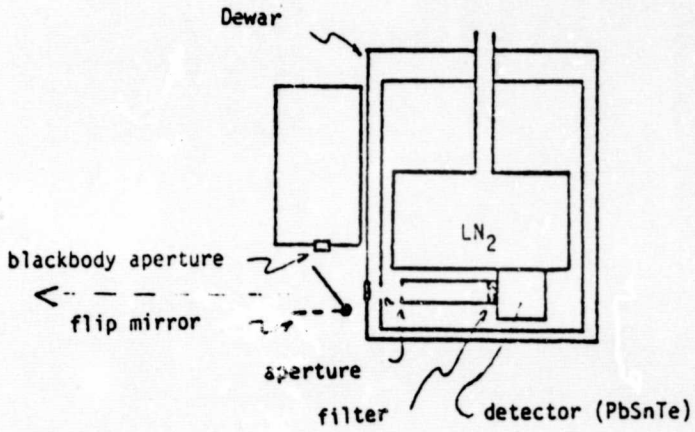

Figure 4. Schematic of whole-sun photometer. It consists of a photovoltaic PbSnTe detector that views the sun through a cold 8.2 - 9.0 μ filter and a Ba Fl_2 entrance window. A flip mirror permits calibration on a blackbody reference source.

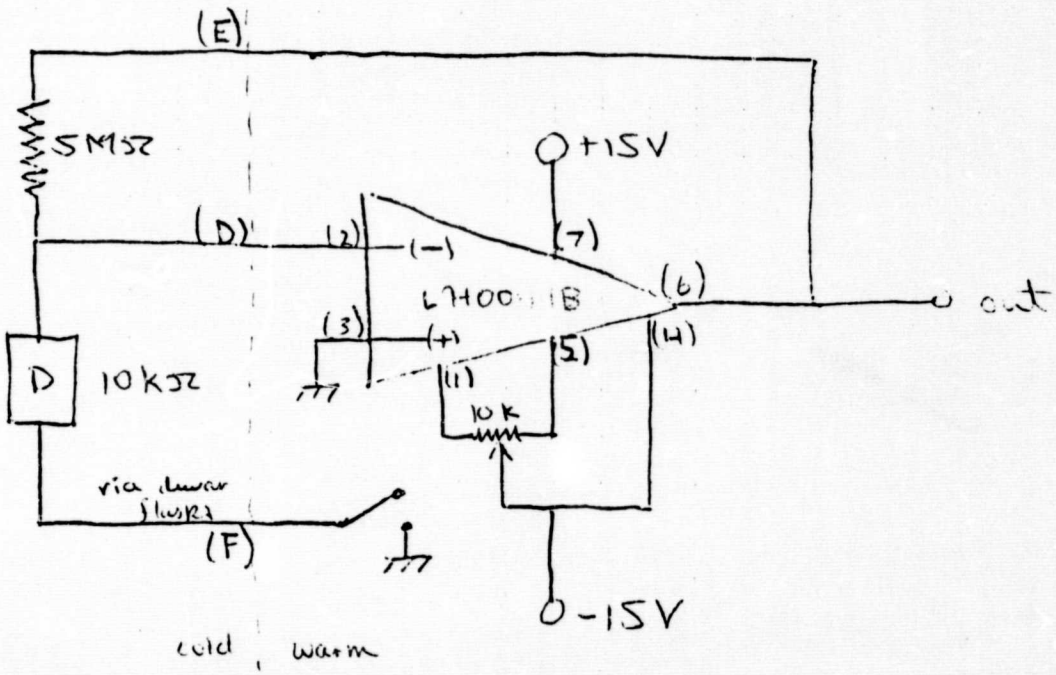

Figure 5. Electronics Configuration.

dimensions with temperature changes about the liquid nitrogen point led to severe output drifts. The problem was remedied by efficiently heat-sinking the filter to the nitrogen flask and optimizing dewar vacuum stability.

The contribution of the entrance window to background flux levels was predicted to be negligible due to its high transmission ($\sim$ 94%) and negligible absorption within the spectral range admitted by the filter. This was indeed found to be the case when window temperature was deliberately varied in the laboratory.

Dewar electronics tests were conducted in a variable temperature environmental chamber, with a constant signal level provided by an internal blocker kept a liquid nitrogen temperature. The drift was found to be 1/10% per degree ambient temperature change. Regulation of electronic component temperature would not be difficult if eventually decided upon.

Isolation of the electronic preamplifier outside of the environmental chamber with the photometer within permitted a test of any internal background loading dependence on temperature changes above the liquid nitrogen baths. The signal level exhibited no change with temperature.

D. Tracking of Solar Disk with Telescope Drive

The infrared photometer is mounted on the Mount Lemmon 60-inch telescope although the optical system of the latter is not put to use. Thus, tracking of the sun throughout the day is possible without the

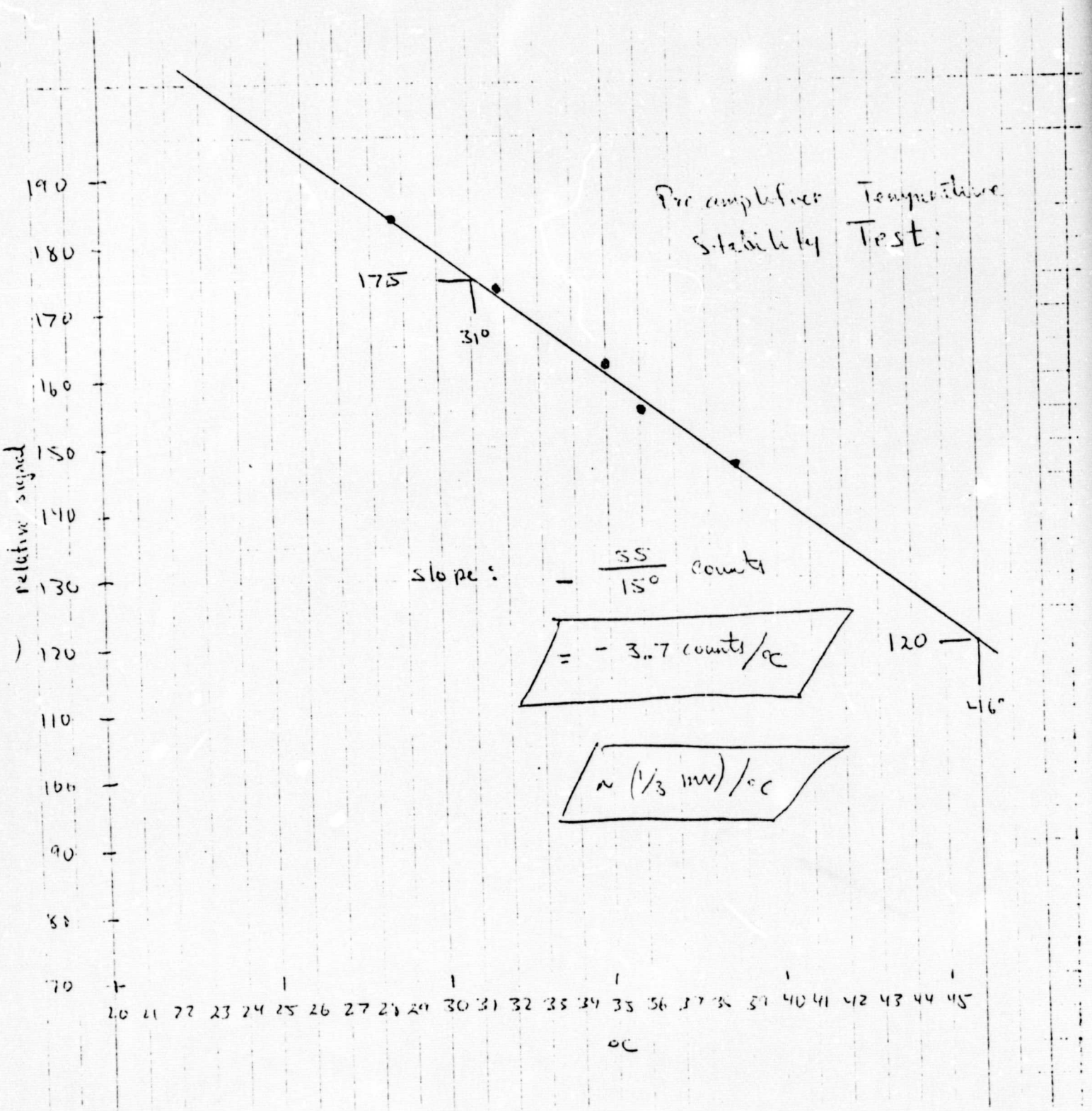

Figure 6. Preamplifier Temperature Stability Test. The regulation of temperature was accomplished through isolation of the preamplifier in a controlled-temperature environmental chamber.

concern of thermal radiation from the reflecting surfaces of the telescope at ten micron wavelengths.

In order for such tracking to be feasible within the precision of our solar irradiance measurements, mis-pointing due to backlash in the telescope drive must be inside a width of the photometer beam profile which is flat within the accuracy of the measurement (typically expressed in several arc minutes for tenths of percent accuracy). Such scans in beam profile made with the large negligible-diffraction apertures (3/8 inch) indicate stability over the range of tracking error. The magnitude of the error in tracking over the course of an observing day has been determined accurately through comparison of beam coordinates at different times, taking into account an hourly update in solar right ascension due to the terrestrial revolution about the sun.

E. Data Acquisition

The acquisition of solar data has been limited to simple procedures up to the present. The analogue output of the preamplifier which correlates directly to solar irradiance at ten microns is supplied to an integrator which averages over ten or 20 second intervals. The integrations are then printed. Solar monitoring initially consisted of sun-pointing for ten minute periods, followed by several minutes of sky-pointing and reference signal determinations, but long-term improvements in the photometer stability have permitted almost total time allotment to the solar spectral flux. Sky signal determinations at

varying zenith angles do permit calculation of a mean sky emission coefficient, but it is not clear that periodic line-of-sight water vapor measurements taken alone would be more beneficial. Water vapor measurements alone would be sufficient in a purely water vapor limited wavelength region, where diurnal ozone variations would be of no import and the mean extinction coefficient determined from the continuous solar signal could be corrected according to short period water vapor fluctuations.

V. OBSERVATIONAL RESULTS

A. Sky Emission Coefficients for Consecutive Observing Days

Sky signal measurements taken over a range of zenith angles provide an immediate determination of the atmospheric emission coefficient. Preliminary observations (Figure 7) give reasonably consistent results from day to day. One should be theoretically able to calculate from such instantaneous emission coefficients an absorption coefficient for the solar radiation, due to the fact that no signal attenuation occurs due to scattering at long infrared wavelengths. This value for the absorption coefficient should correlate well with a simultaneous value of atmospheric water vapor content, in a water-vapor-limited wavelength region.

B. Telescope Tracking Accuracy as Determined From Beam Coordinates

As was discussed in Section IV, telescope tracking limitations pose certain restrictions on how flat the beam profile need be over an

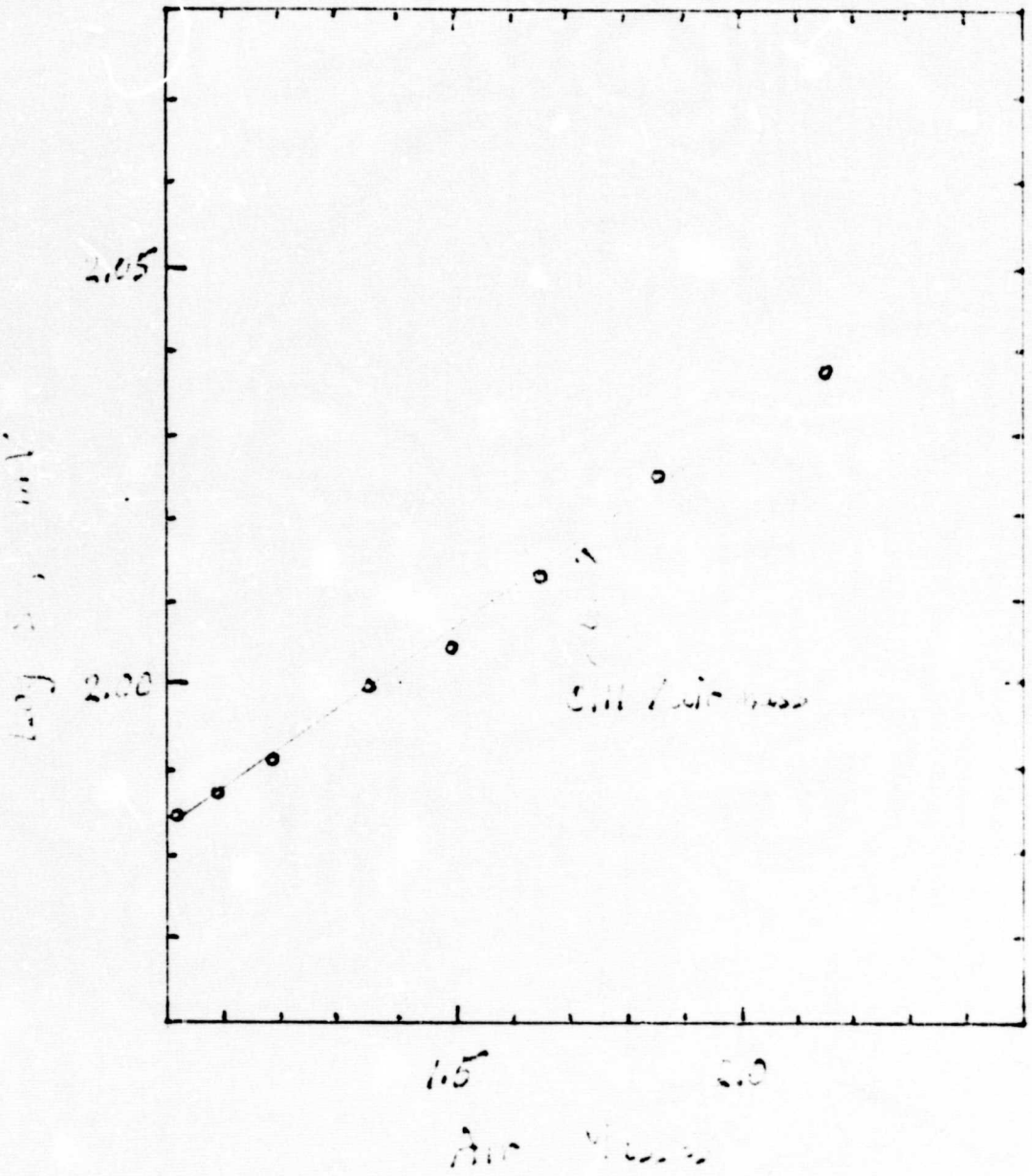

Figure 7. Variation of sky signal with zenith angle. The slope of the emission variation gives information about the extinction coefficient in the 10 micron region; the goodness of fit establishes the nature of the water vapor distribution.

angular range. The tracking accuracy of the telescope drive over the course of an observing day can be determined independently of the right ascension and declination readouts (which would be inaccurate were there any flexure of the telescope at large zenith angles) by noting the pointing of the telescope within the beam at various times. In order to make such a determination, one obtains the instantaneous coordinates of the beam 1/2 power points and pointing location with respect to these. This relative position within the beam should remain constant throughout the day; any deviations (expressed in arc minutes) should be within a range in the beam which is flat.

C. Extinction of Solar Signal with Airmass

The measured value of solar spectral irradiance over a time scale of several hours exhibits its attenuation with airmass. Plots of solar signal against airmass represent a mean extinction which, exhibits some short period variation due to variations in concentration of the atmospheric constituents giving rise to the extinction. Of these, only water vapor is directly measurable. Such extinction plots for various observing days may be compared to the average water vapor content measured over the course of the day. Figure 8 shows a typical extinction plot for 11 micron observations; at this wavelength the extinction is due almost wholly to atmospheric water vapor.

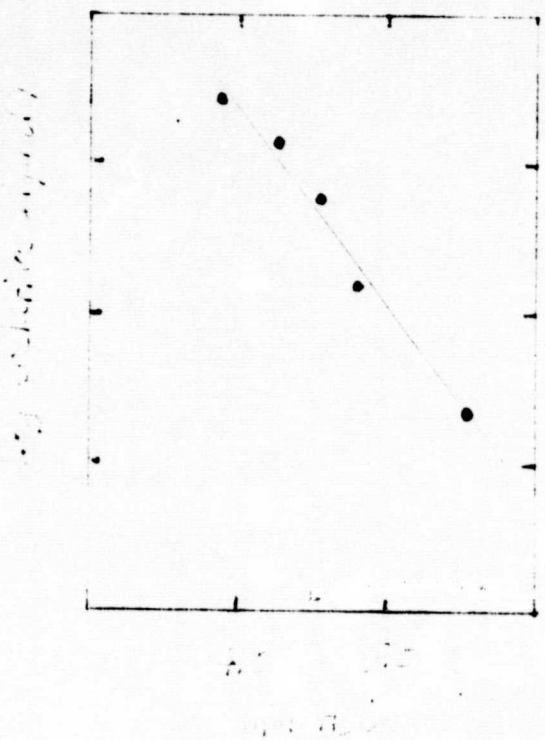

Figure 8. Typical extinction coefficient for 11 micron radiation, plotted against atmospheric line-of-sight water vapor determined by spectral hygrometer. The slope corresponds to 2.1% per mm H_2O extinction.

Observed Periodicities at the One Percent Level

Large scale periodicities (~ 1% of signal level) present in recently acquired data are in the 5 to 10 minute range and appear to be atmospheric in nature. Such an assumption as to their origin will be confirmed by simultaneous observations of the sun at two discrete wavelengths in close proximity to each other, to be conducted in the near future.

VI. CONCLUSIONS

We have described the UCSD solar infrared astronomy program in two phases. The first, completed with the support of NSG-7100, explored various structural features of the solar atmosphere using infrared wavelengths in virtually all ranges accessible from the ground. The second, still in progress, seeks to develop a new means of measuring slow, small-amplitude solar luminosity variations. The 10 μ window has certain unique advantages for this kind of research owing to the nature of atmospheric extinction in the infrared.

Possible sources of variability in solar luminosity include solar-constant variations, variations due to spots and faculae, global oscillations, and potentially flares and other more rapid transient phenomena. To observe any of these will require the development of very stable detection techniques, including means for compensating the effects of variations in the earth's atmosphere. This development work has partially been completed under NSG-7100 and continues with other support.

REFERENCES

Bahng, J., and Schwarzschild, M. 1963, Ap. J., 137, 901.

Bhattacharyya, J. C. 1972, Solar Phys., 24, 274.

Brookes, J. R., Isaak, G. R., and van der Raay, H. B. 1976, Nature, 259, 92.

Christensen-Dalsgaard, J., Dilke, F. W. W., and Gough, D. O. 1974, M.N.R.A.S., 169, 429.

Cowling, T. G. 1941, M.N.R.A.S., 101, 367.

Dilke, F. W. W., and Gough, D. O. 1972, Nature, 240, 262.

Dittmer, P.H., 1977, Ph.D. Thesis (Stanford University)

Edmonds, F. N., Michard, R., and Servajean, R. 1965, Ann. Astrophys., 28, 534.

Evans, J. W., and Michard, R. 1962, Ap. J., 136, 493.

Frazier, E. N. 1966, Pub. Astr. Soc. Pacific, 78, 424.

Frazier, E. N. 1968a, Ap. J., 152, 557.

Frazier, E. N. 1968b, Z. Astrophys., 68, 345.

Gibson, E. G. 1973, The Quiet Sun, Washington, D. C.: NASA.

Gingerich, O., Noyes, R. W., Kalkefen, W., and Cuny, Y. 1971, Solar Phys., 18, 347.

Hill, H. A., Caudell, T. P., and Rosenwald, R. D. 1976, The Proceedings of the Solar and Stellar Pulsation Conference, Los Alamos, New Mexico, ed. A. N. Cox and R. G. Deupree, Los Alamos Report No. LA-6544-C.

Howard, R. 1967, Solar Phys., 2, 3.

Hudson, H. S. 1975, Solar Phys., 45, 69.

Hudson, H., and Lindsey, C. A. 1974, Ap. J. (Letters), 187, L35.

Hudson, H. S., Lindsey, C. A., and Soifer, B. T. 1974, Icarus, 23, 374.

Jensen, E., and Orrall, F. Q. 1963, Ap. J., 138, 252.

Johnson, N. J. 1971, Solar Infrared Limb Profiles, Ph.D. Thesis, University of Michigan.

Ledoux, P., and Walraven, Th. 1958, "Variable Stars," in Handbuch der Physik, Vol. 51, ed. S. Flugge (Berlin: Springer-Verlag), pp. 353-604.

Leibacher, J., and Stein, R. F. 1971, Ap. J. (Letters), 7, 191.

Leighton, R. B., Noyes, R. W., and Simon, G. W. 1962, Ap. J., 135, 474.

Lindsey, C., and Hudson, H. S. 1976, Ap. J., 203, 753.

Livingston, W., Milkey, R., and Slaughter, C. 1977, Ap. J., 211, 281.

Noyes, R. W., and Hall, D. N. B. 1972, Ap. J. (Letters), 176, L89.

Ohki, K.-I., and Hudson, H. S. 1975, Solar Phys., 43, 405.

Severny, A. B., Kotov, V. A., and Tsap, T. T. 1976, Nature, 259, 87.

Thomas, J. H., Clark, P. A., and Clark, A., Jr. 1971, Solar Phys., 16, 51.

Uchida, Y. 1965, Ap. J., 142, 335.

Uchida, Y. 1967, Ap. J., 147, 181.

Ulrich, R. K. 1970, Ap. J., 162, 993.

White, O. R. 1977, The Solar Output and Its Variation, Colorado Associated University Press.

Wolff, C. L. 1972, Ap. J. (Letters), 177, L89.

Wolff, C. L. 1973, Solar Phys., 32, 31.